Available online at www.sciencedirect.com

ScienceDirect

Ceramics International 39 (2013) 9229–9235

CERAMICS INTERNATIONAL

www.elsevier.com/locate/ceramint

Effects of sintering temperature on mechanical properties of 3D mullite fiber (ALF FB3) reinforced mullite composites

Yi Wang*, Haifeng Cheng, Haitao Liu, Jun Wang

Science and Technology on Advanced Ceramic Fibers and Composites Laboratory, College of Aerospace Science and Engineering, National University of Defense Technology, Changsha 410073, China

Received 14 January 2013; received in revised form 8 May 2013; accepted 8 May 2013
Available online 18 May 2013

Abstract

A new method to weaken the interfacial bonding and increase the strength of 3D mullite fiber reinforced mullite matrix (Mu_f/Mu) composites is proposed and tested in this paper. Firstly, Mu_f/Mu composites were fabricated through sol–gel process with varied sintering temperature. Then, the effects of sintering temperature on mechanical properties of the composites were tested. As sintering temperature was raised from 1000 °C to 1300 °C, the three-point flexural strength of the composites firstly decreased from 66.17 MPa to 41.83 MPa, and then increased to 63.17 MPa. In order to explain the relationship between composite strength and sintering temperature, morphology and structure of the mullite fibers and mullite matrix after the same heat-treatment as in the fabrication conditions of the composites were also investigated. Finally, it is concluded that this strength variation results from the combined effects of matrix densification, interfacial bonding and fiber degradation under different sintering temperatures.

Keywords: A. Sol–gel process; C. Mechanical properties; Sintering temperature; Mu_f/Mu composites

1. Introduction

Continuous oxide fiber-reinforced oxide ceramic matrix composites have attracted significant scientific and technological interest in high temperature applications for their excellent properties such as high fracture toughness, damage tolerance, thermal shock and oxidation resistance [1,2]. As one of the most promising oxide ceramic, mullite ($3Al_2O_3 \cdot 2SiO_2$) ceramic has good chemical and high thermal stability, low thermal expansion coefficient ($4.5 \times 10^{-6}\ C^{-1}$) and conductivity (0.06 W cm^{-1} K^{-1}), low dielectric constant ($\varepsilon \approx 7$), and high creep resistance. However, its application is largely limited by the low fracture toughness (about 2.2 MPa $m^{-1/2}$) [3–5]. One way to overcome this limitation is incorporating high-strength continuous ceramic fibers into mullite matrix, and then the activated debonding, delamination, crack deflection, fiber bridging and fiber pull-out mechanisms would lead to a non-linear stress–strain response and high fracture energy [6].

Nevertheless, Mu_f/Mu composites usually have low strength due to the strong interfacial bonding originated from the reaction between fibers and matrix, and the degradation of mullite fibers at high temperatures during the fabrication process [7,8]. Two common ways to weaken the interfacial bonding and thus increase the strength of Mu_f/Mu composites are: (1) introducing interphases or fiber-coating with low toughness, e.g. BN [9], fugitive carbon [10], monazite [11], or porous ZrO_2 [12], by chemical dip-coating or CVD method; (2) adopting porous matrix [13]. Fiber-coating is generally more complex and costly, and it is much more difficult for near-net-shape manufacturing, while the implementation of porous matrix is simpler, more convenient, efficient and economical.

In this paper, we propose a new method to weaken the interfacial bonding–a new diphasic mullite precursor was introduced, and the densification degree of mullite matrix was controlled by varying sintering temperature. The effects of

*Corresponding author. Tel./fax: +86 731 84576440.
E-mail address: wycfcnudt@163.com (Y. Wang).

0272-8842/$ - see front matter
http://dx.doi.org/10.1016/j.ceramint.2013.05.030

Table 1
Properties of ALF mullite fibers.

Type	Diameter (μm)	Density (g/cm^3)	Tensile strength (MPa)	Strength retention (1300 °C, %)	Chemical content (wt%)	Phase content	Highest using temperature (°C)
FB3	10	3.0	1.75	~50	Al_2O_3: 72 SiO_2: 28 B_2O_3:2.0	γ-Al_2O_3, amorphous SiO_2	1400

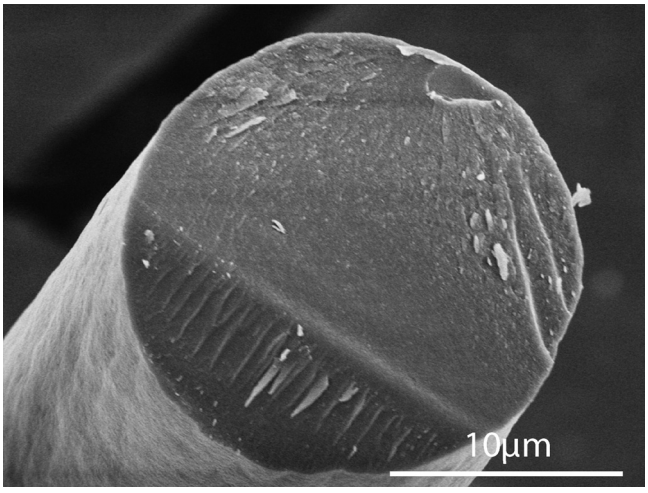

Fig. 1. Fracture surface of the mullite fiber.

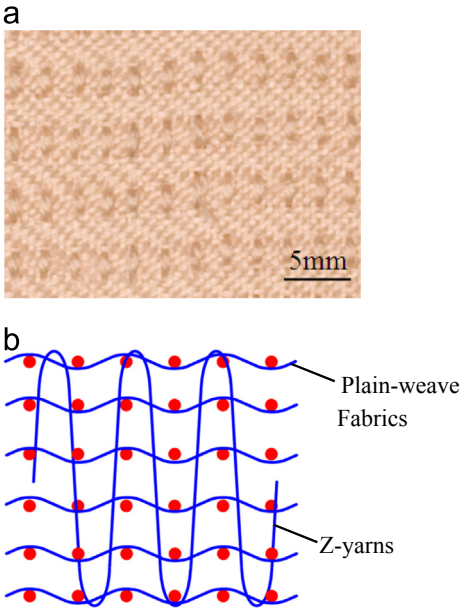

Fig. 2. Photograph (a) and structure (b) of 3D-sewed mullite fiber preform.

sintering temperature on mechanical properties of the composites were tested and discussed in this paper.

2. Experimental procedure

2.1. Materials processing

The reinforcements used to prepare Mu_f/Mu composites were twill-woven mullite fiber fabrics (ALF 3025 T-FB3, from Nitivy ALF Company, Japan), and the properties of the ALF mullite fibers are listed in Table 1. Fracture surface of the mullite fiber is shown in Fig. 1, which demonstrates that the mullite fiber has a circular cross-section, with a diameter of approximately 10 μm. The photograph and structure of the 3D-sewed mullite fiber preform with a fiber volume fraction of about 41.5% are shown in Fig. 2.

Diphasic mullite sol, the precursor of the mullite matrix, was prepared by blending a silica sol and an alumina sol (both from Snowchemical S&T Co., LTD, China) in proportion to their contents in the chemical composition of $3Al_2O_3 \cdot 2SiO_2$ (3/2-mullite) through mechanical stirring lasting for 0.5–1 h. Properties of the silica and alumina sol are listed in Table 2. The density and viscosity of the mullite sol are 1.15 g/cm^3 and 6 mpa s, respectively. The ceramic yield is about 24.1 wt% at 1300 °C and pH is 5.0.

As shown in Fig. 3, the composites were fabricated via sol–gel process, which included vacuum infiltration, gelation and sintering processes. Firstly, the 3D-sewed preforms were vacuum impregnated with mullite sol for 6 h, and then the preforms were gelated at 80 °C for 10 h. Finally, the dried preforms were heated at a rate of 10 °C/min and sintered at 1000 °C, 1200 °C and 1300 °C for 1 h in Ar atmosphere. This sol–gel process was repeated 12 times to densify the composites. The sintering behavior of the mullite matrix was investigated by cold-compacting dried gel powders under the pressure of 100 MPa into Φ40 × 6 mm cylinder samples, which was then sintered at the composites fabrication temperature for 1 h. The mullite fibers having been heat-treated at the composite fabrication temperature for 1 h were also investigated.

Table 2
Properties of silica and alumina sol.

Type	SiO_2 (wt%)	Al_2O_3 (wt%)	pH	Density (g/cm^3)	Ceramic yield (1300 °C, wt%)
Silica sol	24.90	–	4.43	1.12	25.50
Alumina sol	–	20.60	4.00	1.15	17.80

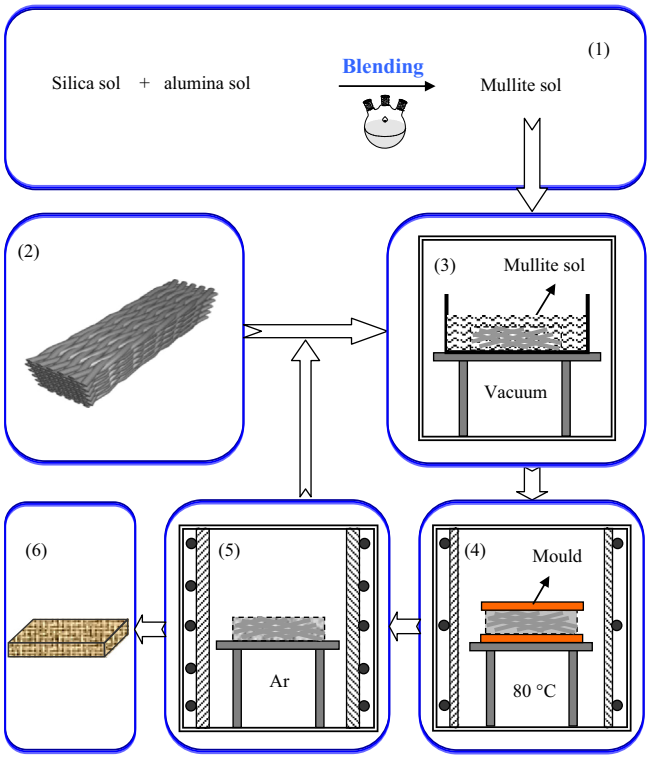

(1) preparation of mullite sol; (2) preparation of 3D mullite fiber preform; (3) infiltration of mullite sol; (4) gelation of mullite; (5) mullization of matrix.

Fig. 3. Fabrication process of 3D Mu_f/Mu composites.

2.2. Materials characterization

Surface morphology of the mullite fibers and mullite matrix after heat-treatment and fracture surface morphology of the Mu_f/Mu composites after mechanical tests were all observed with a scanning electron microscope (SEM, HITACHI FEG S4800). Phases of the mullite fibers and mullite gel powders after heat-treatment were characterized by X-ray diffraction (XRD) analysis using monochromatic CuKa radiation with a D8 ADVANCE diffractometer (Bruker, Germany). A Tecnai F20 high resolution microscope operating at 200 KV was also used to obtain transmission electron microscope (TEM) images.

The density of the samples was measured according to the Archimedes' Laws and their porosity was calculated according to the theoretical density of the composites. Three-point bending tests were carried out at room temperature on samples with size of about $60^l \times 5^w \times 4^t$ mm. The gauge length was 50 mm and cross-head speed was 0.5 mm/min.

3. Results and discussions

3.1. Effects of sintering temperature on the mullite fibers and mullite matrix

The XRD patterns of the mullite fibers are shown in Fig. 4. It can be concluded that the presence of gamma alumina peaks and a wide silica peak at $2\theta \approx 22^\circ$ in as-received fibers, consistent with the data provided by the manufacturer. The

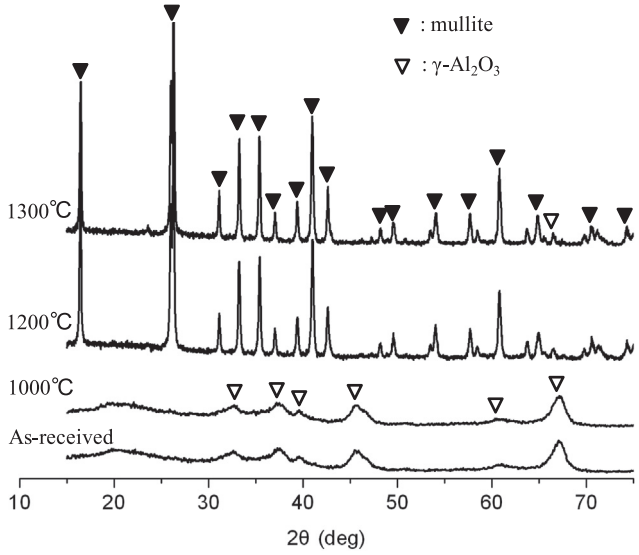

Fig. 4. XRD patterns of mullite fibers after heat-treatment for 1 h at composites fabrication temperature.

mullite phase resulting from the reaction between gamma alumina and amorphous silica appeared at 1200 °C. As temperature kept increasing, the phase structure did not change but mullite grains grew.

Surface morphology of the mullite fibers (Fig. 5) illustrates that as-received fibers are smooth and homogeneous. During the process of heat-treatment, boron oxide in these fibers firstly melted and started to flow, and a large number of liquid ravines were formed. The liquid boron oxide then volatilized, leaving several pores on the fiber surface, although phase transformation and grain growth could also contribute to the formation of these pores. The tensile strength of the mullite fibers stayed stable as the temperature increased from room temperature to 1200 °C, but decreased sharply at 1300 °C, and the strength retention was about 50% of the original value. Strength degradation resulted mainly from the growth of mullite grains. Detailed research on the effects of heat-treatment on mullite fibers was reported in another work [14].

Morphology of the prepared diphasic mullite gel is shown in Fig. 6. It can be seen that spherical silica particles of about 100 nm in diameter are surrounded by rod-shaped boehmite particles with sizes less than $\Phi 20 \times 50$ nm in mullite gel. The HRTEM analysis (Fig. 6b) shows that the silica and boehmite bonded closely, without clear interfaces between them, which is in favor of chemical inter-diffusion and mullite formation [15]. Additionally, polycrystalline boehmite crystals are observed, with inter-planar spacing of 0.197 nm for the (131) lattice planes (PDF-card No. 05-0190).

The XRD patterns of the mullite matrix (Fig. 7) demonstrate that the prepared mullite gel consisted of boehmite and amorphous silica, and the boehmite was decomposed at 500 °C into γ-Al_2O_3, which then transformed into (δ, θ)-Al_2O_3 at 1000 °C [16]. After sintering temperature had reached 1300 °C, the dried gel was crystallized into orthorhombic mullite which had the typical characterization of splitting of the (120) and (210) crystal planes at a 2θ value of about 26° in

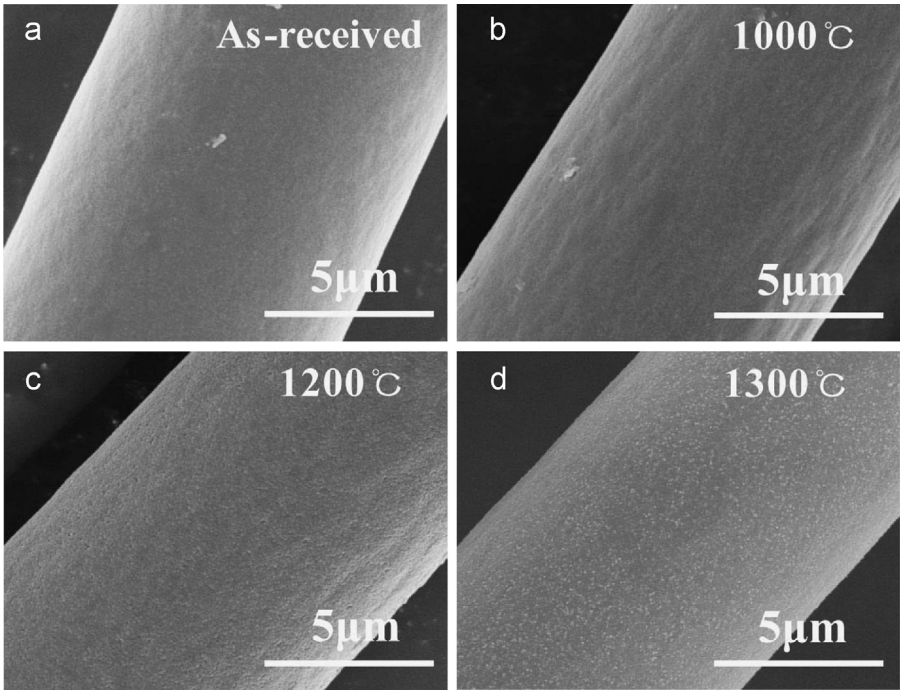

Fig. 5. Surface morphology of mullite fibers after heat-treatment for 1 h at composites fabrication temperature.

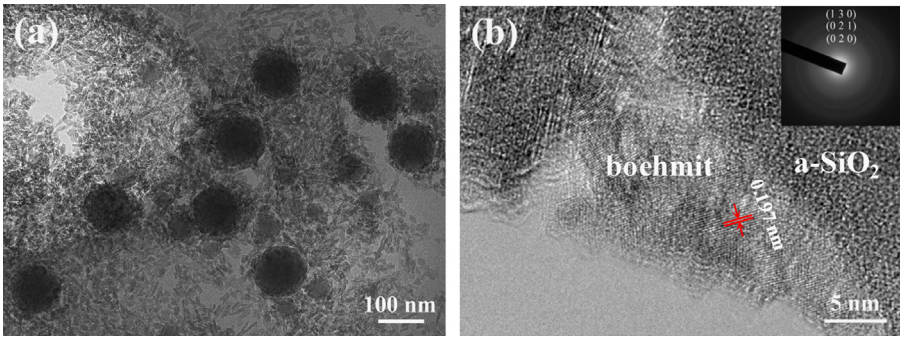

Fig. 6. Morphology of the prepared diphasic mullite gel.

XRD patterns [17]. Apparently, mullite formation temperature was much lower than the alumina-silica solid reaction temperature (~1600 °C) estimated according to the phase equilibrium in alumina and silica systems, and this lowered temperature is largely owing to the homogeneous mixing of alumina and silica particles in mullite sol [18]. Moreover, SiO_2 is also presented in the mullite matrix sintered at 1300 °C.

Fig. 8 shows the optical and SEM images of the mullite matrix after being sintered for 1 h at different temperatures. The optical images indicate that the volume shrinkage of mullite matrix occurred obviously as sintering temperature increased, and the SEM images demonstrate that mullite matrix turned denser with the increase of the sintering temperature.

3.2. *Effects of sintering temperature on the Mu_f/Mu composites*

Properties of the Mu_f/Mu composites are listed in Table 3. It can be concluded that the density of the composites increased from 1.75 g/cm^3 to 2.39 g/cm^3 and their porosity decreased from 33.96% to 17.87% as sintering temperature was raised from 1000 °C to 1300 °C. The measured flexural stress–displacement curves of the composites are shown in Fig. 9. A typical tough fracture behavior appeared for the composites fabricated at 1000 °C, while an obvious brittle failure occurred for the composites fabricated at 1300 °C. The lowest flexural strength of the composites (41.83 MPa) is found on those sintered at 1200 °C. In order to explain the variation of the flexural strength with sintering temperature, fracture morphology of the composites was obtained and the results is shown in Fig. 10.

Fig. 10a shows the existence of many cracks in the matrix sintered at 1000 °C. Thus, the matrix modulus was not large enough to transmit load from the matrix to fibers, although the in-situ fiber strength was very high. As a result, energy dissipation occurred during fiber breaking and subsequent fiber pullout (as shown in Fig. 10b) led to higher strength and also a typical tough fracture behavior. However, for the

composites fabricated at 1200 °C (Fig. 10c,d), many block pores are found in the matrix, and the densification efficiency was highly reduced, resulting in the composite density of only 81.5% of the theoretical value. Moreover, mullite fibers were tightly surrounded by the mullite matrix, suggesting that diffusion and reaction may occur between the fiber and matrix. As mentioned before, the densification degree of the matrix increased with sintering temperature increasing, and Fig. 10c also illustrates the existence of continuous matrix network in the composites. Consequently, the strong interfacial bonding and high matrix porosity may have led to the lowest strength of the composites. On the other hand, Fig. 10e,f reveals less pores in the composites fabricated at 1300 °C, as a result of the densification of the matrix (as shown in Fig. 8f) and the formation of mullite structure in the fibers. Hence, both the strengthened load transmitting from the matrix to fibers and fiber debonding mechanism could contribute to the higher flexural modulus of the composites fabricated at 1300 °C. However, as fiber strength degraded seriously at 1300 °C, the increase of the composite strength was limited.

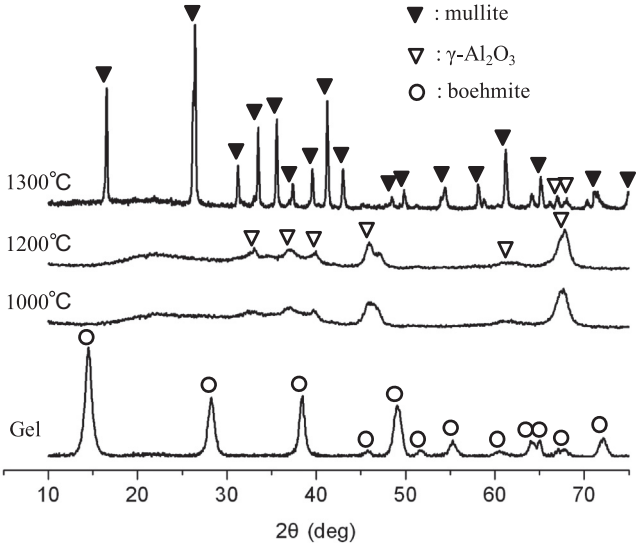

Fig. 7. XRD patterns of mullite matrix after being sintered for 1 h at the composites fabrication temperature.

Although the samples sintered at 1000 °C have the highest strength among all samples, their absolute values are still relatively low compared with those of the composites prepared with proper interphase or porous matrix [19–22]. According to Professor Zok [2,23], high toughness and strength in CFCCs can be achieved by using porous matrix, which promotes uncorrelated failure of the fibers, thus enabling high in-situ fiber strength and energy dissipation during subsequent fiber pullout. Through the use of fine-scale matrix porosity, matrix crack can be deflected effectively. As matrix porosity has been found to have great effect on mechanical properties of porous-matrix, all-oxide ceramic composites, better control of matrix porosity will be resorted to in our pursuit of Mu_f/Mu composites with higher strength. Possible approaches to enhancing matrix modulus and densification could be subsequent heat-treatment or introducing sintering additives such as silica or alumina derived from liquid precursors.

Table 3
Properties of Muf/Mu composites.

Sintering temperature (°C)	Density (g/cm^3)	Porosity (%)	Flexural strength (MPa)	Flexural modulus (GPa)
1000	1.75	33.96	66.17	24.30
1200	2.07	18.50	41.83	42.90
1300	2.39	17.87	63.17	76.20

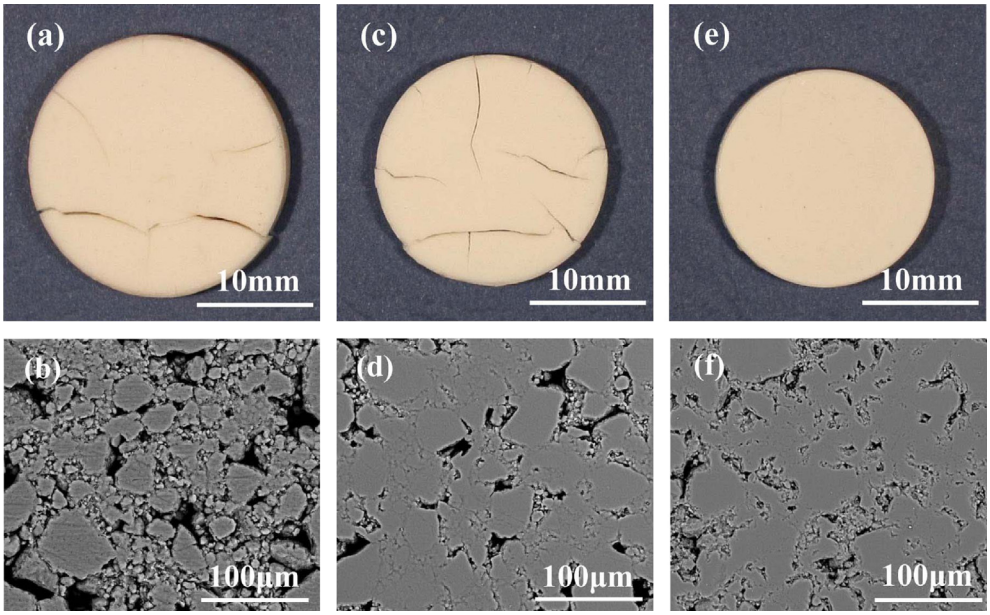

Fig. 8. Optical and SEM images of mullite matrix after being sintered for 1 h at different temperatures: (a)(b) 1000 °C, (c)(d) 1200 °C and (e)(f) 1300 °C.

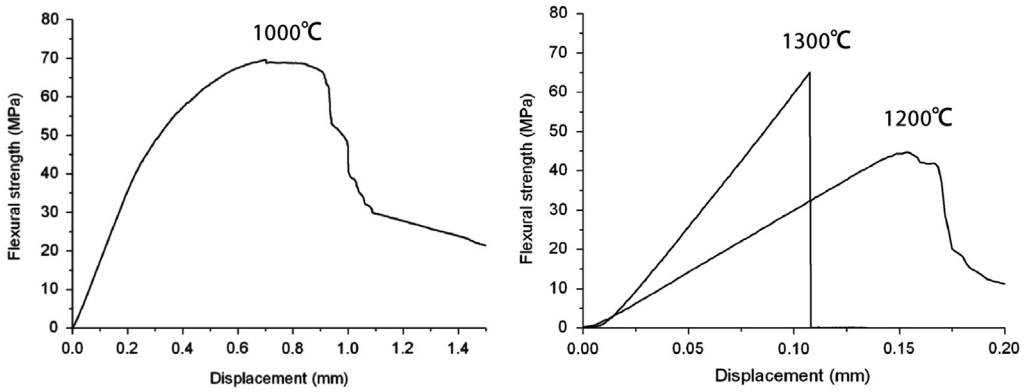

Fig. 9. Experimental flexural stress-displacement curves of Mu_f/Mu composites fabricated at different temperatures.

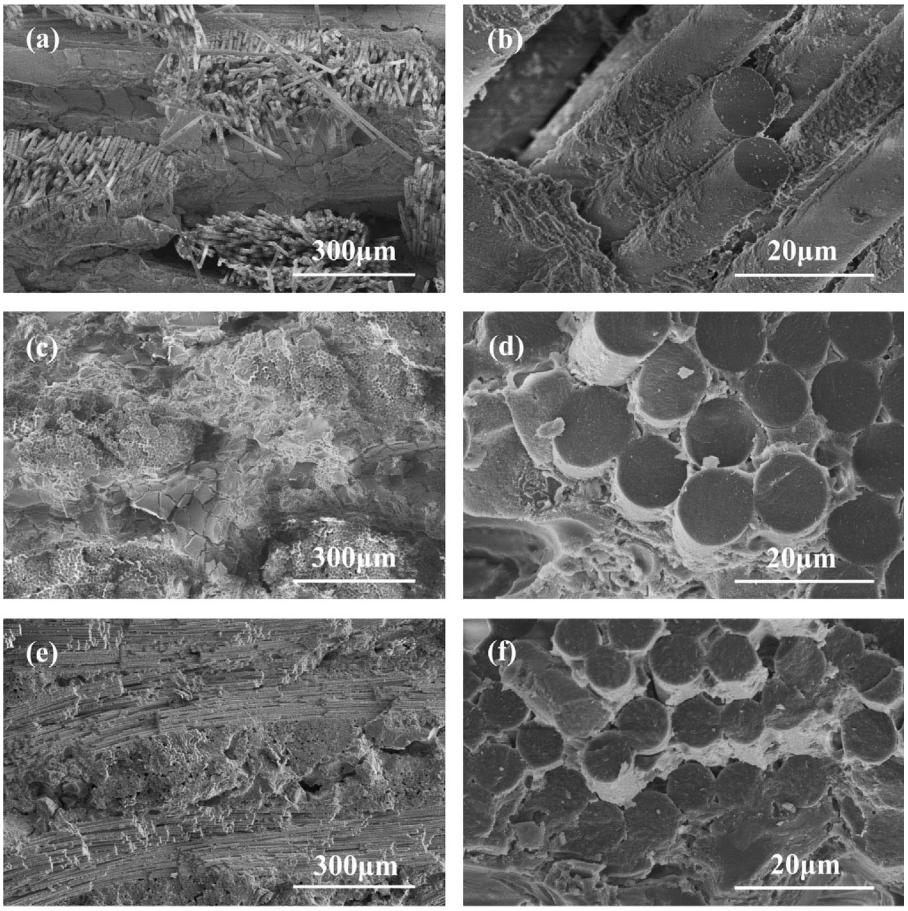

Fig. 10. Fracture morphology of Mu_f/Mu composites fabricated at different temperatures: (a)(b) 1000 °C, (c)(d) 1200 °C and (e)(f) 1300 °C.

4. Conclusions

In this paper, a new method to weaken the interfacial bonding and increase the strength of Mu_f/Mu composites is proposed, in which a new diphasic mullite sol is introduced in the sol–gel process and the sintering temperature is adjusted to control the densification degree of mullite matrix. With this method, 3D Mu_f/Mu composites were successfully prepared, and the effects of sintering temperature on the mullite fibers, mullite matrix and Mu_f/Mu composites were all investigated.

Results show that the mullite sol prepared by mixing the silica sol and alumina sol had high homogeneity and could form orthorhombic mullite at 1300 °C. Phase transformation and grain growth led to strength degradation for mullite fibers after heat-treatment at 1200 °C and 1300 °C. Three-point flexural strength of the composites were firstly decreased from 66.17 MPa to 41.83 MPa and then increased to 63.17 MPa as sintering temperature was raised from 1000 °C to 1300 °C, and the lowest strength was found in the composites fabricated at 1200 °C. This phenomenon is explained as the result of three

mechanisms varying with sintering temperatures: matrix densification, interfacial bonding and fiber degradation.

Acknowledgments

The authors appreciate the financial support of the National Natural Science Foundation of China (51202291), Aid Program for the Innovative Group of National University of Defense Technology, and the Aid program for Science and Technology Innovative Research Team in Higher Educational Institutions of Hunan Province.

References

[1] L.P. Zawada, R.S. Hay, S.S. Lee, J. Staehler, Characterization and high-temperature mechanical behavior of an oxide/oxide composite, Journal of the American Ceramic Society 86 (2003) 981–990.
[2] F.W. Zok, Developments in oxide fiber composites, Journal of the American Ceramic Society 89 (2006) 3309–3324.
[3] H. Schneider, S. Komarneni (Eds.), Mullite, WILEY-VCH Verlag GmbH & Co. KGaA, Weinheim, 2005.
[4] H. Schneider, J. Schreuer, B. Hildmann, Structure and properties of mullite—a review, Journal of the European Ceramic Society 28 (2008) 329–344.
[5] I.A. Aksay, D.M. Dabbs, M. Sarikaya, Mullite for structural, electronic, and optical applications, Journal of the American Ceramic Society 74 (1991) 2343–2358.
[6] C. Kaya, E.G. Butler, A. Selcuk, et al., Mullite (Nextel^{TM} 720) fibre-reinforced mullite matrix composites exhibiting favourable thermomechanical properties, Journal of the European Ceramic Society 22 (2002) 2333–2342.
[7] E. Mouchon, P. Colomban, Oxide ceramic matrix/oxide fibre woven fabric composites exhibiting dissipative fracture behavior, Composites 26 (1995) 175–182.
[8] M. Schmücker, F. Flucht, P. Mechnich, Degradation of oxide fibers by thermal overload and environmental effects, Materials Science and Engineering: A 557 (2012) 10–16.
[9] M. Schmücker, H. Schneider, Thermal degradation of fiber coatings in mullite-fiber-reinforced mullite composites, Journal of the American Ceramic Society 80 (1997) 2136–2140.
[10] J.H. Weaver, J. Yang, F.W. Zok, Control of interface properties in oxide composites via fugitive coatings, Journal of the American Ceramic Society 91 (2008) 4003–4008.
[11] J.B. Davis, D.B. Marshall, P.E.D. Morgan, Monazite-containing oxide/oxide composites, Journal of the European Ceramic Society 20 (2000) 583–587.
[12] D. Desimone, D.D. Jayaseelan, W.E. Lee, A.R. Boccaccini, Development of ZrO_2 interfaces for all-oxide composites, Composites Science and Technology 72 (2012) 197–203.
[13] F.W. Zok, C.G. Levi, Mechanical properties of porous-matrix ceramic composites, Advanced Engineering Materials 3 (2001) 15–23.
[14] Y. Wang, H.F. Cheng, H.T. Liu, J. Wang, Microstructure and room temperature mechanical properties of mullite fibers after heat-treatment at elevated temperatures, Materials Science and Engineering: A (2013) in press.
[15] L.S. Cividanes, T.M.B. Campos, L.A. Rodrigues, et al., Review of mullite synthesis routes by sol–gel method, Journal of Sol–Gel Science and Technology 55 (2010) 111–125.
[16] H. Schneider, L. Merwin, A. Sebald, Mullite formation from non-crystalline precursors, Journal of Materials Science 27 (1992) 805–812.
[17] E.R. de Sola, F.J. Serrano, F.J. Torres, et al., An X-ray powder diffraction study of the microstructural evolution on heating 3:2 and 2:1 mullite single-phase gels, Crystal Research and Technology 41 (2006) 1036–1044.
[18] J.A. Pask, X.W. Zhang, A.P. Tomsia, Effect of sol–gel mixing on mullite microstructure and phase equilibria in the α-$A1_2O_3$–SiO_2 system, Journal of the American Ceramic Society 70 (1987) 704–707.
[19] Y.H. Bao, P.S. Nicholson, $AlPO_4$-coated mullite/alumina fiber reinforced reaction-bonded mullite composites, Journal of the European Ceramic Society 28 (2008) 3041–3048.
[20] K.K. Chawla, H. Liu, J.J. Ruschc, S. Sambasivan, Microstructure and properties of monazite ($LaPO_4$) coated saphikon fiber/alumina matrix composites, Journal of the European Ceramic Society 20 (2000) 551–559.
[21] M.G. Holmquist, F.F. Lange, Processing and properties of a porous oxide matrix composite reinforced with continuous oxide fibers, Journal of the American Ceramic Society 86 (2003) 1733–1740.
[22] E.A.V. Carelli, H. Fujita, J.Y. Yang, F.W. Zok, Effects of thermal aging on the mechanical properties of a porous-matrix ceramic composite, Journal of the American Ceramic Society 85 (2002) 595–602.
[23] M.A. Mattoni, J.Y. Yang, C.G. Levi, F.W. Zok, Effects of matrix porosity on the mechanical properties of a porous-matrix, all-oxide ceramic composite, Journal of the American Ceramic Society 84 (2001) 2594–2602.